Viscometric Functions for a Dilute Solution of Polymers in a Good Solvent

J. Ravi Prakash

Department of Chemical Engineering, Indian Institute of Technology, Madras, India 600 036

Hans Christian Öttinger*

Department of Materials, Institute of Polymers, ETH Zürich, CH-8092 Zürich, Switzerland

Received September 29, 1998; Revised Manuscript Received December 29, 1998

ABSTRACT: A dilute polymer solution is modeled as a suspension of noninteracting Hookean dumbbells, and the effect of excluded volume is taken into account by incorporating a narrow Gaussian repulsive potential between the beads of each dumbbell. The narrow Gaussian potential is a means of regularizing a δ-function potential: it tends to the δ-function potential in the limit of the width parameter μ going to zero. Exact predictions of viscometric functions in simple shear flow are obtained with the help of a retarded motion expansion and by Brownian dynamics simulations. It is shown that for relatively small *nonzero* values of μ, the presence of excluded volume causes a *swelling* of the dumbbell at equilibrium and *shear thinning* in simple shear flow. On the other hand, a δ-function excluded-volume potential does not lead to either swelling or to shear thinning. Approximate viscometric functions, obtained by assuming that the bead-connector vector is described by a Gaussian nonequilibrium distribution function, are found to be accurate above a threshold value of μ, for a given value of the strength of excluded-volume interaction, z. A first-order perturbation expansion reveals that the Gaussian approximation is exact to first order in z. The predictions of an alternative quadratic excluded-volume potential suggested earlier by Fixman (*J. Chem. Phys.* **1966**, *45*, 785, 793) are also compared with those of the narrow Gaussian potential.

1. Introduction

The fact that two parts of a polymer chain cannot occupy the same place at the same time because of their finite volume has been recognized in the polymer literature for many years now as being an extremely important microscopic phenomenon that governs the macroscopic behavior of polymer solutions.[7,8,20] Like hydrodynamic interaction, the *excluded-volume* effect influences the properties of polymer solutions even in the limit of extremely long chains because it is responsible for segments remote from each other along the polymer chain interacting with each other.

While the effect of excluded volume on static properties of polymer solutions has been widely studied, there have been very few attempts at examining its influence on properties far from equilibrium. Excluded-volume effects can be incorporated into bead−spring chain models for polymer solutions in a relatively straightforward manner by adding the excluded-volume interaction force between a particular bead and all of the other beads in the chain (pairwise) to the other potential forces that are acting on the bead. A noteworthy aspect of this approach is the kind of repulsive potential that is adopted to represent the excluded-volume interactions. In static theories of polymer solutions, the excluded-volume interaction is typically assumed to be a very short range δ-function potential.

Fixman[9] and more recently Ahn et al.[1] have attempted to predict the rheological properties of dilute polymer solutions by approximately incorporating the effects of both hydrodynamic interaction and excluded volume in a self-consistent manner into a bead−spring chain model. (Ahn et al. also include finitely extensible springs in place of Hookean springs). To obtain a solvable model, Fixman[9] used a repulsive quadratic excluded-volume potential in place of a δ-function potential. This leads to a tractable model because the bead-connector vectors are then described by a Gaussian nonequilibrium distribution function. Results obtained with the quadratic excluded-volume potential have, however, not been compared so far with the results of other models for the excluded-volume potential.

Andrews et al.[2] have recently carried out a numerical study of the influence of excluded-volume interactions on rheological and rheooptical properties of dilute solutions, with the help of Brownian dynamics and configuration-biased Monte Carlo simulations. A bead−spring chain model, with "Fraenkel" springs between beads and a Morse potential to represent excluded-volume interactions, was used to model the flexible polymer molecule. Attention was largely confined to the prediction of properties in elongational flow and transient shear flow.

The predictions of their theories in the limit of long chains have not been considered by Fixman,[9] Ahn et al.,[1] or Andrews et al.[2] On the other hand, the universal character of excluded-volume effects have been studied using renormalization group theory methods based on kinetic theory models (with a δ-function excluded-volume potential) by Öttinger and co-workers.[14,23]

While the work of Andrews et al.[2] is based on Brownian dynamics simulations, the accuracy of the other *approximate* treatments of excluded volume cited above has not been tested by comparison with Brownian dynamics simulations (which are an ideal tool for testing approximations for nonlinear effects). This is in contrast to the situation that exists for kinetic theory models that only incorporate hydrodynamic-interaction effects, where extensive comparisons between the exact results of Brownian dynamics simulations and various approximations have been made.[21,22]

10.1021/ma981534b CCC: $18.00
Published on Web 03/02/1999

It is the purpose of this paper to examine the influence of the excluded-volume effect on the rheological properties of a dilute polymer solution by using a *narrow Gaussian potential* to describe the excluded-volume interactions. Because the narrow Gaussian potential tends to the δ-function potential in the limit of a parameter μ (that describes the width of the potential) going to zero, it provides a means of evaluating results obtained with a singular δ-function potential. Compared to the δ-function potential, analytical calculations are not significantly harder with the narrow Gaussian potential; quite often, upon setting $\mu = 0$ at the end of a calculation, the predictions of a δ-function potential can be obtained. Furthermore, because Brownian dynamics simulations cannot be performed with a δ-function potential, simulations carried out with the narrow Gaussian potential for small values of the parameter μ provide a means of asymptotically obtaining the predictions of a δ-function potential model.

Any molecular theory that seeks to describe the dynamics of polymers in good solvents must simultaneously incorporate both the microscopic phenomena of hydrodynamic interaction and excluded volume, because hydrodynamic-interaction effects have been shown to have an unavoidable influence on the dynamic behavior of polymer solutions. However, it would be difficult to explore the consequences of such a theory for two reasons. First, the incorporation of hydrodynamic interaction would lead to the complication of multiplicative noise. Second, because Brownian dynamics simulations for long chains would be extremely computationally intensive, any approximations that are developed can only be tested for very short chains. For these reasons and because this is a preliminary investigation, we examine excluded-volume effects independently from hydrodynamic-interaction effects and confine attention here to a Hookean dumbbell model for the polymer. This enables the careful evaluation of various approximations. It is hoped that, in the future, the best approximation can be used for chains with both hydrodynamic interaction and excluded volume, with the ultimate objective of calculating universal properties predicted in the long chain limit.

It must be noted that unlike in the case of the quadratic potential, the use of the narrow Gaussian potential does not lead to exact solvability. Indeed, as has been observed in earlier treatments of other nonlinear microscopic phenomenon such as hydrodynamic interaction and internal viscosity, it is found that it is not possible to obtain an analytical solution valid at all shear rates. As a result, retarded-motion expansions, Brownian dynamics simulations, and perturbative and nonperturbative approximation procedures are used in this work to obtain the material functions predicted by the narrow Gaussian potential.

An important consequence of using the narrow Gaussian potential is that the nature of Fixman's quadratic excluded-volume potential can be explored. Predictions of Fixman's quadratic excluded-volume potential in simple shear flow will be compared with the predictions of the narrow Gaussian potential.

The outline of this paper is as follows. In section 2, the basic equations required to discuss the dynamics of Hookean dumbbells in good solvents are derived. In section 3, the various material functions considered in this paper are defined. A retarded-motion expansion for the stress tensor, for arbitrary excluded-volume potentials, is derived in section 4, and power-series expansions for the material functions in simple shear flow are obtained. Section 5 is devoted to examining the consequences of describing the excluded-volume interaction with a narrow Gaussian potential. In section 5.1, expressions for the material functions predicted with this potential at zero shear rate are obtained by using the retarded-motion expansion. The formulation of a Brownian dynamics simulation algorithm is discussed in section 5.2, and a Gaussian approximation for the configurational distribution function is introduced in section 5.3. In section 5.4, a first-order perturbation expansion in the strength of the excluded-volume interaction is derived. Fixman's theory for dumbbells is presented in section 6, in terms of the framework adopted for the rest of the discussion in this paper. The results of the various exact and approximate treatments are compared and discussed in section 7, and the principal conclusions of the paper are summarized in section 8.

2. Basic Equations

The Hookean dumbbell model represents a macromolecule by a mechanical model that consists of two identical beads connected by a spring. The solvent in which the beads are suspended is assumed to be Newtonian, and attention is restricted to flows which have a homogeneous velocity field, i.e., of the form $\mathbf{v} = \mathbf{v}_0 + \kappa(t)\cdot\mathbf{r}$, where $\mathbf{v}_0$ is a constant vector, $\kappa(t)$ is a traceless tensor, and $\mathbf{r}$ is the position vector with respect to a laboratory-fixed frame of reference. The instantaneous position of the beads are specified by bead-position vectors $\mathbf{r}_1$ and $\mathbf{r}_2$.

This paper examines the consequence of introducing an excluded-volume interaction between the beads of the dumbbell, so that the total potential experienced by the beads, ϕ, is the sum of the spring potential S, and the excluded-volume potential E. The force on bead ν due to this potential, $\mathbf{F}_\nu^{(\phi)}$, is then given by $\mathbf{F}_\nu^{(\phi)} = -\partial\phi/\partial\mathbf{r}_\nu$. For Hookean springs, the spring potential is given by $S = {}^1/_2HQ^2$, where H is the spring constant. Two forms of the excluded-volume potential are considered in this work, namely, the narrow Gaussian potential and Fixman's quadratic potential. These are discussed in greater detail subsequently. Here, we summarize the governing equations that are valid for an arbitrary choice of the excluded-volume potential E.

For homogeneous flows, the configurational distribution function $\psi(\mathbf{Q}, t)$ depends only on the internal configuration of the dumbbell, specified by the bead-connector vector $\mathbf{Q} = \mathbf{r}_2 - \mathbf{r}_1$, and not on the center of mass. The quantity $\psi(\mathbf{Q}, t)\,d\mathbf{Q}$ is then the probability that at time t the dumbbell has a configuration in the range from $\mathbf{Q}$ to $\mathbf{Q} + d\mathbf{Q}$. Using the framework of polymer kinetic theory,[5] one can show that the distribution function $\psi(\mathbf{Q}, t)$, in the presence of excluded volume, satisfies the following *diffusion equation*

$$\frac{\partial\psi}{\partial t} = -\frac{\partial}{\partial\mathbf{Q}}\cdot\left\{(\kappa\cdot\mathbf{Q})\psi - \frac{2}{\zeta}\psi\frac{\partial\phi}{\partial\mathbf{Q}} - \frac{2k_BT}{\zeta}\frac{\partial\psi}{\partial\mathbf{Q}}\right\} \qquad (1)$$

where ζ is the bead friction coefficient (i.e., $\zeta = 6\pi\eta_s a$ for spherical beads with radius a, in a solvent with viscosity η_s), k_B is Boltzmann's constant, and T is the absolute temperature. The stress tensor, $\boldsymbol{\tau}$, in a polymer solution is considered to be given by the sum of two contributions, $\boldsymbol{\tau} = \boldsymbol{\tau}^s + \boldsymbol{\tau}^p$, where $\boldsymbol{\tau}^s$ is the contribution

from the solvent, and $\boldsymbol{\tau}^p$ is the polymer contribution. Since the solvent is assumed to be Newtonian, $\boldsymbol{\tau}^s = -\eta_s\dot{\boldsymbol{\gamma}}$, where $\dot{\boldsymbol{\gamma}}$ is the rate of strain tensor, $\dot{\boldsymbol{\gamma}} = (\nabla\mathbf{v})(t) + (\nabla\mathbf{v})^\dagger(t)$. The rheological properties of a dilute polymer solution may thus be obtained by calculating the polymer contribution to the stress tensor, $\boldsymbol{\tau}^p$. For a dumbbell model in the presence of excluded volume, it is given by Kramers' expression[5]

$$\boldsymbol{\tau}^p = -n\left\langle \mathbf{Q}\frac{\partial\phi}{\partial\mathbf{Q}}\right\rangle + nk_BT\,\mathbf{1} \tag{2}$$

Here, n is the number density of polymers, and angular brackets represent averaging with respect to the configurational distribution function $\psi(\mathbf{Q}, t)$.

For both of the excluded-volume potentials considered here, it will turn out that calculation of the second moment $\langle\mathbf{QQ}\rangle$ is necessary in order to evaluate the average in eq 2. A time evolution equation for the second moment can be obtained by multiplying the diffusion equation, eq 1, by $\mathbf{QQ}$ and integrating over all configurations

$$\frac{\mathrm{d}}{\mathrm{d}t}\langle\mathbf{QQ}\rangle = \boldsymbol{\kappa}\cdot\langle\mathbf{QQ}\rangle + \langle\mathbf{QQ}\rangle\cdot\boldsymbol{\kappa}^T + \frac{4k_BT}{\zeta}\mathbf{1} - \frac{2}{\zeta}\left[\left\langle \mathbf{Q}\frac{\partial\phi}{\partial\mathbf{Q}}\right\rangle + \left\langle\frac{\partial\phi}{\partial\mathbf{Q}}\mathbf{Q}\right\rangle\right] \tag{3}$$

It proves convenient for subsequent calculations to introduce the following dimensionless variables

$$t^* = \frac{t}{\lambda_H},\quad \mathbf{Q}^* = \sqrt{\frac{H}{k_BT}}\mathbf{Q},\quad \boldsymbol{\kappa}^* = \lambda_H\boldsymbol{\kappa},\quad \phi^* = S^* + E^* \tag{4}$$

where $\lambda_H = (\zeta/4H)$ is the familiar time constant, $S^* = S/k_BT = (1/2)\mathbf{Q}^{*2}$ and $E^* = E/k_BT$ are the nondimensional Hookean spring potential and the nondimensional excluded-volume potential, respectively. Note that θ-solvent values of a typical time scale (λ_H) and a typical length scale ($\sqrt{k_BT/H}$) are used for the purpose of nondimensionalization, regardless of the form of the excluded-volume potential.

The intramolecular force is expected to be in the direction of the bead-connector vector. Therefore, it can be written in terms of nondimensional variables as

$$\frac{\partial\phi^*}{\partial\mathbf{Q}^*} = H^*(Q^*)\mathbf{Q}^* \tag{5}$$

where $H^*(Q^*)$ is an arbitrary function of the magnitude of $\mathbf{Q}^*$. As a result, the diffusion equation, eq 1, in terms of nondimensional variables, is given by

$$\frac{\partial\psi}{\partial t^*} = -\frac{\partial}{\partial\mathbf{Q}^*}\cdot\left\{\boldsymbol{\kappa}^*\cdot\mathbf{Q}^* - \frac{1}{2}H^*(Q^*)\mathbf{Q}^*\right\}\psi + \frac{1}{2}\frac{\partial}{\partial\mathbf{Q}^*}\cdot\frac{\partial\psi}{\partial\mathbf{Q}^*} \tag{6}$$

and Kramers' expression, eq 2, assumes the form

$$\frac{\boldsymbol{\tau}^p}{nk_BT} = -\langle H^*(Q^*)\mathbf{Q}^*\mathbf{Q}^*\rangle + \mathbf{1} \tag{7}$$

and the second-moment equation, eq 3, becomes

$$\frac{\mathrm{d}}{\mathrm{d}t^*}\langle\mathbf{Q}^*\mathbf{Q}^*\rangle = \boldsymbol{\kappa}^*\cdot\langle\mathbf{Q}^*\mathbf{Q}^*\rangle + \langle\mathbf{Q}^*\mathbf{Q}^*\rangle\cdot\boldsymbol{\kappa}^{*T} - \langle H^*(Q^*)\mathbf{Q}^*\mathbf{Q}^*\rangle + \mathbf{1} \tag{8}$$

Equation 8 is in general not a closed equation for the second moments because it depends on the form of the function $H^*(Q^*)$ (i.e., on the choice of excluded-volume potential).

On examination of eqs 7 and 8, it is straightforward to see that the second-moment equation, eq 8, is nothing but the Giesekus expression for the stress tensor

$$\frac{\boldsymbol{\tau}^p}{nk_BT} = \frac{\mathrm{d}}{\mathrm{d}t^*}\langle\mathbf{Q}^*\mathbf{Q}^*\rangle - \boldsymbol{\kappa}^*\cdot\langle\mathbf{Q}^*\mathbf{Q}^*\rangle - \langle\mathbf{Q}^*\mathbf{Q}^*\rangle\cdot\boldsymbol{\kappa}^{*T} \tag{9}$$

Although the equations derived in this section are valid for arbitrary homogeneous flows, in this paper, we confine attention to the prediction of rheological properties in simple shear flows, defined in the section below.

3. Simple Shear Flows

3.1. Steady Simple Shear Flow. Steady simple shear flows are described by a tensor $\boldsymbol{\kappa}$ which has the following matrix representation in the laboratory-fixed coordinate system

$$\boldsymbol{\kappa} = \dot{\gamma}\begin{pmatrix}0&1&0\\0&0&0\\0&0&0\end{pmatrix} \tag{10}$$

where $\dot{\gamma}$ is the constant shear rate.

The three independent material functions used to characterize such flows are the viscosity, η_p, and the first and second normal stress difference coefficients, Ψ_1 and Ψ_2, respectively. These functions are defined by the following relations[4]

$$\tau^p_{xy} = -\dot{\gamma}\eta_p,\quad \tau^p_{xx} - \tau^p_{yy} = -\dot{\gamma}^2\Psi_1,\quad \tau^p_{yy} - \tau^p_{zz} = -\dot{\gamma}^2\Psi_2 \tag{11}$$

3.2. Small-Amplitude Oscillatory Shear Flow. A transient experiment that is used often to characterize polymer solutions is small-amplitude oscillatory shear flow, where the tensor $\boldsymbol{\kappa}(t)$ is given by

$$\boldsymbol{\kappa}(t) = \dot{\gamma}_0\cos\omega t\begin{pmatrix}0&1&0\\0&0&0\\0&0&0\end{pmatrix} \tag{12}$$

Here, $\dot{\gamma}_0$ is the amplitude, and ω is the frequency of oscillations in the plane of flow. The polymer contribution to the shear stress, τ^p_{yx}, depends on time through the relation[4]

$$\tau^p_{yx} = -\eta'(\omega)\,\dot{\gamma}_0\cos\omega t - \eta''(\omega)\,\dot{\gamma}_0\sin\omega t \tag{13}$$

where η' and η'' are the material functions characterizing oscillatory shear flow. They are represented in a combined form as the complex viscosity, $\eta^* = \eta' - i\eta''$.

In the linear viscoelastic flow regime, the stress tensor is described by the linear constitutive relation

$$\boldsymbol{\tau}^p(t) = -\int_{-\infty}^{t}\mathrm{d}s\;G(t-s)\,\dot{\boldsymbol{\gamma}}(s) \tag{14}$$

where $G(t)$ is the relaxation modulus. As a result, for oscillatory shear flows with a small amplitude $\dot{\gamma}_0$, expressions for the real and imaginary parts of the complex viscosity can be found in terms of the relaxation

modulus from the expression

$$\eta^* = \int_0^\infty G(s)\, e^{-i\omega s}\, ds \tag{15}$$

Note that the zero shear rate viscosity $\eta_{p,0}$ and the zero shear rate first normal stress difference $\Psi_{1,0}$, which are linear viscoelastic properties, can be obtained from the complex viscosity in the limit of vanishing frequency

$$\eta_{p,0} = \lim_{\omega\to 0} \eta'(\omega), \quad \Psi_{1,0} = \lim_{\omega\to 0} \frac{2\eta''(\omega)}{\omega} \tag{16}$$

4. Retarded-Motion Expansion

A retarded-motion expansion for the stress tensor, derived previously for the FENE (finitely extensible nonlinear elastic) dumbbell model,[5] can be adapted to the present instance by recognizing that the FENE spring potential (as indeed any choice of excluded-volume potential) is but a particular example of a connector-force potential between the beads of the dumbbell. In this section, we briefly summarize the development of a retarded-motion expansion for an arbitrary choice of the excluded-volume potential. Details of the derivation may be found in Bird et al.[5]

We seek a solution of the diffusion equation, eq 6, whereby the configurational distribution function, $\psi(\mathbf{Q}, t)$, can be written as a product of an equilibrium contribution and a flow contribution

$$\psi(\mathbf{Q}, t) = \psi_{eq}(\mathbf{Q})\phi_{fl}(\mathbf{Q}, t) \tag{17}$$

The governing equation for the flow contribution $\phi_{fl}(\mathbf{Q}, t)$

$$\frac{\partial \phi_{fl}}{\partial t^*} = -\left\{\frac{\partial \phi_{fl}}{\partial \mathbf{Q}^*} - \phi_{fl}\frac{\partial \phi^*}{\partial \mathbf{Q}^*}\right\}\cdot\boldsymbol{\kappa}^*\cdot\mathbf{Q}^* + \frac{1}{2}\left\{\frac{\partial}{\partial \mathbf{Q}^*}\cdot\frac{\partial \phi_{fl}}{\partial \mathbf{Q}^*} - \frac{\partial \phi_{fl}}{\partial \mathbf{Q}^*}\cdot\frac{\partial \phi^*}{\partial \mathbf{Q}^*}\right\} \tag{18}$$

can be obtained by substituting eq 17 into the diffusion equation, eq 6, and exploiting the fact that the equilibrium distribution function is given by

$$\psi_{eq}(\mathbf{Q}) = N_{eq}\, e^{-\phi^*} \tag{19}$$

where N_{eq} is the normalization constant.

Regardless of the form of the excluded-volume potential, at steady state, an exact solution to eq 18 can be found for all homogeneous *potential* flows.[5] For more general homogeneous flows, however, it is necessary to seek a perturbative solution. The flow contribution, $\phi_{fl}(\mathbf{Q}, t)$, is assumed to be expandable in a power series in the velocity gradients

$$\phi_{fl}(\mathbf{Q}, t) = 1 + \phi_1 + \phi_2 + \phi_3 + \ldots \tag{20}$$

where ϕ_k is of order k in the velocity gradient.

Partial differential equations governing each of the ϕ_k may be obtained by substituting eq 20 into eq 18 and equating terms of like order. Following the procedure suggested in Bird et al.,[5] one can judiciously guess the specific forms for the functions ϕ_k by noting that each of these functions must have certain properties. The form of the function ϕ_1 which satisfies these requirements is

$$\phi_1 = \frac{1}{2}\mathbf{Q}^*\cdot\dot{\boldsymbol{\gamma}}\cdot\mathbf{Q}^* \tag{21}$$

while the form of ϕ_2 can be guessed to be

$$\phi_2 = {}^1/_8(\mathbf{Q}^*\cdot\dot{\boldsymbol{\gamma}}\cdot\mathbf{Q}^*)^2 - {}^1/_{60}\langle\mathbf{Q}^{*4}\rangle_{eq}\,\mathrm{tr}(\dot{\boldsymbol{\gamma}}\cdot\dot{\boldsymbol{\gamma}}) + A^*(Q^*)\mathbf{Q}^*\cdot\dot{\boldsymbol{\gamma}}\cdot\boldsymbol{\omega}\cdot\mathbf{Q}^* \tag{22}$$

where $\langle\ \rangle_{eq}$ denotes an average with $\psi_{eq}(\mathbf{Q})$, $\boldsymbol{\omega}$ is the vorticity tensor, defined here as $\boldsymbol{\omega} = \boldsymbol{\kappa}^* - \boldsymbol{\kappa}^{*T}$, and the scalar function $A^*(Q^*)$ obeys the following second-order differential equation

$$\frac{d^2A^*}{dQ^{*2}} + \left(\frac{6}{Q^*} - H^*(Q^*)Q^*\right)\frac{dA^*}{dQ^*} - 2A^*(Q^*)H^*(Q^*) = 1 \tag{23}$$

It is difficult to suggest boundary conditions for eq 23 other than to say that the solution must be such that $\psi(\mathbf{Q}, t)$ is bounded. In the case of FENE springs, it is possible to explicitly obtain the particular solution of a similar second-order differential equation.

It is clear from eq 9 that at steady state, the stress tensor can be found once $\langle\mathbf{Q}^*\mathbf{Q}^*\rangle$ is known. The second moment $\langle\mathbf{Q}^*\mathbf{Q}^*\rangle$ can be found correct to second order in velocity gradients by using the power-series expansion, eq 20, for $\phi_{fl}(\mathbf{Q}, t)$, and the specific forms for ϕ_1 and ϕ_2 in eqs 21 and 22, respectively. This leads to the following expression for the stress tensor, correct to third order in velocity gradients,

$$\begin{aligned}-\frac{\boldsymbol{\tau}^p}{nk_BT} &= \frac{\lambda_H}{3}\left(\frac{H}{k_BT}\right)\langle Q^2\rangle_{eq}\{\dot{\boldsymbol{\gamma}}\} + \frac{\lambda_H^2}{30}\left(\frac{H}{k_BT}\right)^2\langle Q^4\rangle_{eq}\{2\dot{\boldsymbol{\gamma}}^2 - (\dot{\boldsymbol{\gamma}}\cdot\boldsymbol{\omega} - \boldsymbol{\omega}\cdot\dot{\boldsymbol{\gamma}})\} \\ &+ \frac{\lambda_H^3}{105}\left(\frac{H}{k_BT}\right)^3\langle Q^6\rangle_{eq}\left\{\frac{3}{4}\mathrm{tr}(\dot{\boldsymbol{\gamma}}\cdot\dot{\boldsymbol{\gamma}})\dot{\boldsymbol{\gamma}} - \frac{1}{2}(\dot{\boldsymbol{\gamma}}^2\cdot\boldsymbol{\omega} - \boldsymbol{\omega}\cdot\dot{\boldsymbol{\gamma}}^2)\right\} \\ &- \frac{\lambda_H^3}{180}\left(\frac{H}{k_BT}\right)^3\langle Q^4\rangle_{eq}\langle Q^2\rangle_{eq}\{\mathrm{tr}(\dot{\boldsymbol{\gamma}}\cdot\dot{\boldsymbol{\gamma}})\dot{\boldsymbol{\gamma}}\} \\ &+ \frac{\lambda_H^3}{30}\left(\frac{H}{k_BT}\right)^2\langle Q^4A^*\rangle_{eq}\{(\dot{\boldsymbol{\gamma}}^2\cdot\boldsymbol{\omega} - \boldsymbol{\omega}\cdot\dot{\boldsymbol{\gamma}}^2) \\ &+ \boldsymbol{\omega}\cdot(\dot{\boldsymbol{\gamma}}\cdot\boldsymbol{\omega} - \boldsymbol{\omega}\cdot\dot{\boldsymbol{\gamma}}) - (\dot{\boldsymbol{\gamma}}\cdot\boldsymbol{\omega} - \boldsymbol{\omega}\cdot\dot{\boldsymbol{\gamma}})\cdot\boldsymbol{\omega}\} + \ldots\end{aligned} \tag{24}$$

The Cayley−Hamilton theorem has been used to eliminate the term $\dot{\boldsymbol{\gamma}}^3$ in eq 24, and an isotropic term that does not affect the rheological properties has been dropped.

The stress tensor in simple shear flow, for small values of the nondimensional shear rate $\lambda_H\dot{\gamma}$, can be found by substituting eq 10 for the rate of strain tensor in eq 24. By use of the definitions of the viscometric functions in eq 11, the following power-series expansions are obtained,

$$\begin{aligned}\frac{\eta_p}{\lambda_H nk_BT} &= \frac{1}{3}\left(\frac{H}{k_BT}\right)\langle Q^2\rangle_{eq} + \left\{\frac{2}{15}\left(\frac{H}{k_BT}\right)^2\langle Q^4A^*\rangle_{eq} + \right. \\ &\left.\frac{1}{70}\left(\frac{H}{k_BT}\right)^3\langle Q^6\rangle_{eq} - \frac{1}{90}\left(\frac{H}{k_BT}\right)^3\langle Q^4\rangle_{eq}\langle Q^2\rangle_{eq}\right\}(\lambda_H\dot{\gamma})^2 + \ldots\end{aligned} \tag{25}$$

$$\frac{\Psi_1}{\lambda_H^2 nk_BT} = \frac{2}{15}\left(\frac{H}{k_BT}\right)^2\langle Q^4\rangle_{eq} + \ldots \tag{26}$$

Clearly, eq 26 indicates that one must expand to higher orders in velocity gradients before the shear rate dependence of the first normal stress difference can be obtained. Zero shear rate properties, however, can be obtained from eqs 25 and 26.

5. The Narrow Gaussian Potential

In the static theory of polymer solutions, it is common to represent the dimensionless excluded-volume potential, between two points on the polymer chain separated by a nondimensional distance $\mathbf{Q}^*$, with the Dirac δ-function

$$E^*(\mathbf{Q}^*) = (2\pi)^{3/2} z\delta(\mathbf{Q}^*) \tag{27}$$

where $z = v(H/2\pi k_B T)^{3/2}$ is a nondimensional parameter which represents the strength of the excluded-volume interaction and v (which has the dimensions of volume) is called the "excluded-volume parameter".[8] The parameter z is frequently used in theories that incorporate excluded volume, as it is considered to be the appropriate parameter to be used in perturbation expansions. As mentioned earlier, excluded-volume interactions are taken into account in this work by means of a narrow Gaussian potential.[15] The narrow Gaussian potential has the following form in terms of nondimensional variables,

$$E^*(\mathbf{Q}^*) = \frac{z}{\mu^3} \exp\left(-\frac{1}{2}\frac{Q^{*2}}{\mu^2}\right) \tag{28}$$

It is clear from eq 28 that the nondimensional parameter μ controls the extent of the excluded-volume interaction, and as $\mu \to 0$, the narrow Gaussian potential tends to the δ-potential. The narrow Gaussian potential, as mentioned earlier, serves as a means of regularizing the singular δ-potential and, consequently, permits the evaluation of results obtained with a δ-potential.

With excluded-volume interactions described by the narrow Gaussian potential, the function $H^*(Q^*)$, which appears in eq 5 for the nondimensional force between the beads of the dumbbell, is given by

$$H^*(Q^*) \equiv H_G^*(Q^*) = 1 - \left(\frac{z}{\mu^5}\right) \exp\left[-\frac{Q^{*2}}{2\mu^2}\right] \tag{29}$$

The complex form of this function implies that the diffusion equation, eq 6, cannot be solved exactly analytically to obtain the nonequilibrium configurational distribution function $\psi(\mathbf{Q}, t)$. Furthermore, the time evolution equation for the second moments, eq 8, is not a closed equation for the second moments because it involves the higher-order moment $\langle H_G^*(Q^*)\mathbf{Q}^*\mathbf{Q}^*\rangle$ on the right-hand side. As a result, perturbative methods, nonperturbative approximation procedures, or numerical schemes must be used to obtain the material functions predicted by the narrow Gaussian potential.

5.1. Zero Shear Rate Properties. The viscosity and the first normal stress difference predicted by the narrow Gaussian potential at low shear rates can be obtained from the eqs 25 and 26, respectively, once the equilibrium averages that occur in these expressions are evaluated. For the narrow Gaussian potential, the equilibrium distribution function is given by eq 19, with the excluded-volume contribution to the nondimensional potential ϕ^* given by eq 28. We denote the various nondimensional moments of the equilibrium distribution for a narrow Gaussian potential by

$$q_m \equiv \left(\frac{H}{k_B T}\right)^m \langle Q^{2m}\rangle_{eq}; \quad m = 1, 2, 3, \ldots \tag{30}$$

In order to obtain the viscosity at nonzero shear rates, it is necessary to find the function A^* that satisfies the second-order differential equation, eq 23 [with $H^*(Q^*) = H_G^*(Q^*)$]. Unlike in the case of an FENE dumbbell, it has not been possible to obtain the particular solution to eq 23. As a result, attention is confined here to obtaining the zero shear rate predictions of the narrow Gaussian potential

$$\frac{\eta_{p,0}}{\lambda_H n k_B T} = \frac{1}{3} q_1 \tag{31}$$

$$\frac{\Psi_{1,0}}{\lambda_H^2 n k_B T} = \frac{2}{15} q_2 \tag{32}$$

for which only the moments q_1 and q_2 are required. Alternative methods will be used in sections 5.2−5.4 to obtain the shear rate dependence of the viscometric functions.

The nondimensional equilibrium moments q_1 and q_2 can be obtained exactly, as will be shown in section 5.1.1 below. The need to calculate equilibrium moments is also frequently encountered in static theories of polymer solutions. In these theories, as mentioned earlier, it is common to represent excluded-volume interactions with a δ-function excluded-volume potential and, furthermore, to obtain universal predictions by considering the limit of long chains. The Hamiltonian then typically involves two singular objects, making it impossible to evaluate equilibrium moments exactly. The most successful approach so far toward approximately evaluating these moments has been to develop a perturbation expansion in the parameter z and to use renormalization group methods to refine the results of the perturbation calculation.[7,8] An alternative and simpler nonperturbative route is the uniform-expansion model.[8] The use of the narrow Gaussian potential, albeit in the simple context of dumbbells, provides an opportunity to compare the results of these approximate models with the exact solution. The rigorous solution is discussed in section 5.1.1 below, and the perturbation-expansion and the uniform-expansion models are discussed in sections 5.1.2 and 5.1.3, respectively.

5.1.1. Exact Solution. It is straightforward to show that the moments q_m are given by the ratio of two integrals, $q_m = (I_m/I_0)$, where

$$I_j \equiv \int_0^\infty Q^{*2j+2} \exp\{-(1/2)Q^{*2} - E^*\}\, dQ^*; \quad j = 0, 1, 2, \ldots \tag{33}$$

In the limit of $\mu \to 0$ and $\mu \to \infty$, these integrals can be evaluated analytically. Consider the quantities

$$p_j(Q^*) \equiv Q^{*2j+2} \exp\left\{-\frac{1}{2}Q^{*2} - E^*\right\}$$

which are the integrands for the integrals I_j, and

$$R_j(Q^*) \equiv Q^{*2j+2} \exp\left\{-\frac{1}{2}Q^{*2}\right\}$$

Now, $p_j(0) = R_j(0) = 0$, for all values of μ. At any nonzero value of Q^*, it is clear from eq 28 that

$$p_j(Q^*) \rightarrow R_j(Q^*) \quad \text{as } \mu \rightarrow 0 \text{ or } \infty$$

In other words, for all values of Q^*, the quantities $p_j(Q^*)$ tend *pointwise* to $R_j(Q^*)$ as μ tends to zero or to infinity. Furthermore, for all values of μ, it can be shown that $p_j(Q^*)$ are bounded functions of Q^* on $[0, \infty[$. It then follows from a theorem of the calculus[6] that

$$q_m \rightarrow \frac{\int_0^\infty Q^{*2m+2} \exp\left\{-\frac{1}{2}Q^{*2}\right\} dQ^*}{\int_0^\infty Q^{*2} \exp\left\{-\frac{1}{2}Q^{*2}\right\} dQ^*} \quad \text{as } \mu \rightarrow 0 \text{ or } \infty$$

As a result, the asymptotic values of q_m for $\mu \rightarrow 0$ and $\mu \rightarrow \infty$ are found to be *independent* of z and are equal to the θ-solvent values,

$$q_1 = 3;\ q_2 = 15;\ q_3 = 105;\ \ldots$$

This implies, from eqs 31 and 32, that the use of a δ-function potential to represent excluded-volume interactions leads to the prediction of zero shear rate properties in good solvents which are identical to those in θ-solvents.

Away from these limiting values of μ, i.e., at nonzero finite values of μ, the integrals of I_j can be found by numerical quadrature. Here, they have been evaluated using a routine given in Press et al.[11] for the integration of an exponentially decaying integrand. Discussion of zero shear rate property predictions in this case is taken up in section 7.

5.1.2. Perturbation Expansion. Static theories for polymer solutions indicate that accounting for excluded-volume interactions with a δ-function potential leads to the prediction of a *swelling* (i.e., an increase in the mean-square end-to-end distance) of the polymer chain, which is in close agreement with experimental observations.[7,8] In the case of a Hookean dumbbell, however, we have seen above that the use of a δ-function potential to account for the presence of excluded volume (which corresponds to the limit $\mu \rightarrow 0$) does not lead to any change in the prediction of equilibrium moments when compared to the θ-solvent case. It is worthwhile therefore to examine the nature of the perturbation expansion in z and compare it to the results of the exact calculation.

Upon the expansion of e^{-E^*} in a power series, the integral I_j has the form

$$I_j \equiv \int_0^\infty dQ^* \sum_{n=0}^{\infty} u_n(Q^*);\ j = 0, 1, 2, \ldots \qquad (34)$$

where

$$u_n(Q^*) = \frac{(-1)^n}{n!} Q^{*2j+2}\, e^{-1/2Q^{*2}} [E^*(Q^*)]^n \qquad (35)$$

In order to carry out a term-by-term integration of the functional series $\sum_{n=0}^{\infty} u_n(Q^*)$ in eq 34, it is necessary for the series to be *uniformly convergent* on $[0, \infty[$. For all values of z and $\mu \neq 0$, uniform convergence can be established with the help of the Weierstrass M test.[6] Therefore, a term-by-term integration in eq 34 can be carried out, *except* when $\mu = 0$. Assuming that $\mu \neq 0$ and performing the integration in eq 34, one obtains

$$I_j = 2^{j+1/2}\Gamma\left(j + \frac{3}{2}\right) \sum_{n=0}^{\infty} \frac{(-1)^n}{n!} \left(\frac{z}{\mu^3}\right)^n \frac{\mu^{2j+3}}{(n+\mu^2)^{j+3/2}};$$
$$j = 0, 1, 2, \ldots \qquad (36)$$

Consider the moment q_1, which is undoubtedly the most interesting physical moment. By use of the perturbation expansion for I_j, q_1 is given by the ratio $q_1 = 3(S_1/S_0)$, where S_0 and S_1 are defined by

$$S_0 = \sum_{n=0}^{\infty} \frac{(-1)^n}{n!} \left(\frac{z}{\mu^3}\right)^n \frac{\mu^3}{(n+\mu^2)^{3/2}}$$

$$S_1 = \sum_{n=0}^{\infty} \frac{(-1)^n}{n!} \left(\frac{z}{\mu^3}\right)^n \frac{\mu^5}{(n+\mu^2)^{5/2}} \qquad (37)$$

If only the first-order perturbation term is retained, one obtains

$$q_1 = 3\left(1 + \frac{z}{(1+\mu^2)^{5/2}}\right) \qquad (38)$$

Curiously, the limit $\mu \rightarrow 0$ can be carried out in this case. It leads to a result which is in line with static theories, which indicate a finite nonvanishing effect due to the presence of δ-potential excluded-volume interactions. However, such a limit cannot be carried out if higher-order terms are retained, because both of the sums S_0 and S_1 diverge as $\mu \rightarrow 0$. In static theories, higher-order perturbation expansions are obtained by *dropping* divergent terms, as they are postulated not to matter. These divergent terms arise from products of the δ-potential for the *same* pair of interacting beads. In dumbbells, these are the only kind of beads present. As a result, there is no meaningful or mathematically consistent way of going beyond first-order perturbation theory for dumbbells in the limit $\mu \rightarrow 0$.

Note that both of the series S_0 and S_1 are alternating series. Furthermore, for given values of z and μ, the terms decrease monotonically for large-enough values of n. It follows then, from the Leibnitz criterion for alternating series,[3] that both S_0 and S_1 converge for all values of z and $\mu \neq 0$. This suggests that, even though it is not possible to switch the integral and summation in eq 34 for $\mu = 0$, the value of q_1 at $\mu = 0$ can be found by setting it equal to the limit of $q_1(\mu)$ as $\mu \rightarrow 0$. We shall see in section 7 that such a limiting process is infeasible because it becomes numerically impossible to evaluate the sums in eqs 37 for small-enough values of μ.

5.1.3. Uniform-Expansion Model. The uniform-expansion model seeks to approximate the average $\langle X \rangle_{eq}$ of any quantity $X(\mathbf{Q})$, with $\langle X \rangle'_{eq}$, where $\langle\ \rangle'_{eq}$ denotes an average with the Gaussian equilibrium distribution function,

$$\psi'_{eq}(\mathbf{Q}) = N'_{eq} \exp\left\{-\frac{3}{2b'^2}Q^2\right\} \qquad (39)$$

with $N'_{eq} = [3/2\pi b'^2]^{3/2}$. The aim is to find the parameter b' that leads to the best possible approximation. As may be expected, this depends on the quantity $X(\mathbf{Q})$ that is averaged. The motivation behind the uniform-expansion

model and details regarding the calculation of b' are given in appendix A. Because the equilibrium distribution function in the absence of excluded volume is Gaussian, this assumption expects the equilibrium distribution to remain Gaussian upon the incorporation of excluded volume, albeit with an increased end-to-end vector.

If we define u_m such that $u_m \equiv (H/k_BT)^m\langle Q^{2m}\rangle'_{eq}$, then clearly u_m is the uniform-expansion model approximation for q_m. Uniform-expansion model predictions of the zero shear rate properties are given by eqs 31 and 32, with q_m replaced by u_m. Results of material properties obtained by numerical quadrature, and by the uniform-expansion model, are discussed in section 7.

5.2. Brownian Dynamics Simulations. Development of the retarded-motion expansion has proved useful in obtaining exact expressions for the zero shear rate properties. At nonzero shear rates, exact predictions of the viscometric functions can be obtained by solving the Ito stochastic differential equation,

$$d\mathbf{Q}^* = \left[\kappa^* - \frac{1}{2}H^*(Q^*)\mathbf{1}\right]\cdot\mathbf{Q}^*\,dt + d\mathbf{W} \qquad (40)$$

which corresponds to the nondimensional diffusion equation, eq 6, and in which **W** is a three-dimensional Wiener process.

For the narrow Gaussian potential, because $H^*(Q^*) = H_G^*(Q^*)$, eq 40 is nonlinear. As a result, it cannot be solved analytically. Two different Brownian dynamics simulation algorithms have been adopted here for the numerical solution of eq 40. Both schemes use a second-order predictor−corrector algorithm with time-step extrapolation.[15] The first scheme obtains steady-state expectations by the simulation of a single long trajectory and is based on the assumption of ergodicity.[15] It has been used to obtain results at equilibrium and for large values of the shear rate. A second algorithm, which employs a variance reduction procedure, has been used at low values of the shear rate, because the variance for the viscometric functions is found to be relatively large at these shear rates. Reduction in the variance is obtained by following a scheme suggested by Wagner and Öttinger.[18] The scheme, which constructs an ensemble of trajectories over several relaxation times, from start-up of flow to steady-state, essentially consists of subtracting the rheological properties obtained from a parallel equilibrium simulation. While this does not change the average values of the properties, it significantly reduces the fluctuations, because the fluctuations are virtually the same at zero and small shear rates. The results of these simulation algorithms are discussed in section 7.

5.3. The Gaussian Approximation. The main obstacle (in the configuration space of the dumbbell) to obtaining the rheological properties predicted by a narrow Gaussian potential is that the second-moment equation is not a closed equation. A closure problem has also been encountered earlier in treatments of the phenomenon of hydrodynamic interaction and internal viscosity, where it has been shown that an accurate approximation can be obtained by assuming that the nonequilibrium configurational distribution function is a Gaussian distribution.[16,17,19,21,22] In this section, a similar systematic approximation procedure for the treatment of excluded-volume interactions described by a narrow Gaussian potential is introduced.

The assumption that $\psi(\mathbf{Q}, t)$ is a Gaussian distribution,

$$\psi(\mathbf{Q}, t) = \frac{1}{(2\pi)^{3/2}}\frac{1}{\sqrt{\det\langle\mathbf{QQ}\rangle}}\exp\left\{-\frac{1}{2}\mathbf{Q}\cdot\langle\mathbf{QQ}\rangle^{-1}\cdot\mathbf{Q}\right\} \qquad (41)$$

makes the second-moment equation, eq 8, a closed equation, because the higher-order moment $\langle H_G^*(Q^*)\mathbf{Q}^*\mathbf{Q}^*\rangle$ can be expressed in terms of the second moment. When this reduction is performed, it can be shown that the Gaussian approximation leads to the following closed second-moment equation,

$$\frac{d}{dt^*}\langle\mathbf{Q}^*\mathbf{Q}^*\rangle = \kappa^*\cdot\langle\mathbf{Q}^*\mathbf{Q}^*\rangle + \langle\mathbf{Q}^*\mathbf{Q}^*\rangle\cdot\kappa^{*T} - \langle\mathbf{Q}^*\mathbf{Q}^*\rangle + \frac{z}{\sqrt{\det[\langle\mathbf{Q}^*\mathbf{Q}^*\rangle + \mu^2\,\mathbf{1}]}}\boldsymbol{\Pi} + \mathbf{1} \qquad (42)$$

where

$$\boldsymbol{\Pi} = [\langle\mathbf{Q}^*\mathbf{Q}^*\rangle + \mu^2\,\mathbf{1}]^{-1}\cdot\langle\mathbf{Q}^*\mathbf{Q}^*\rangle$$

It is also straightforward to show that upon the introduction of the Gaussian approximation, the Giesekus expression for the stress tensor has the form

$$\frac{\boldsymbol{\tau}^p}{nk_BT} = -\langle\mathbf{Q}^*\mathbf{Q}^*\rangle + \frac{z}{\sqrt{\det[\langle\mathbf{Q}^*\mathbf{Q}^*\rangle + \mu^2\,\mathbf{1}]}}\boldsymbol{\Pi} + \mathbf{1} \qquad (43)$$

The steady-state viscometric functions (defined by eq 11) can therefore be found once eq 42 is solved for $\langle\mathbf{Q}^*\mathbf{Q}^*\rangle$.

It is worth examining the nature of the polymer contribution to the stress tensor. In the limit $\mu \to 0$, $\boldsymbol{\Pi}$ reduces to **1**, and as a result, the presence of excluded volume only makes an indirect contribution through its influence on the second moment $\langle\mathbf{Q}^*\mathbf{Q}^*\rangle$. This follows from the fact that an isotropic contribution to the stress tensor makes no difference to the rheological properties of the polymer solution. On the other hand, for nonzero values of μ, the rheological properties are also affected directly by excluded volume.

Under the Gaussian approximation, linear viscoelastic properties can be obtained by deriving a first-order codeformational memory integral expansion for the stress tensor. The tensor $\langle\mathbf{Q}^*\mathbf{Q}^*\rangle$ is expanded, in terms of deviations from its isotropic equilibrium solution, up to first order in velocity gradient,

$$\langle\mathbf{Q}^*\mathbf{Q}^*\rangle = \alpha^2(\mathbf{1} + \epsilon + \ldots) \qquad (44)$$

where the parameter α (commonly called the swelling ratio) is defined by

$$\alpha^2 = \frac{\langle Q^2\rangle_{eq}}{\langle Q^2\rangle_{0,eq}} \qquad (45)$$

Here, $\langle Q^2\rangle_{0,eq} = (3k_BT/H)$ is the mean-square end-to-end distance in the absence of excluded volume. Clearly, α represents the *equilibrium* swelling of the polymer chain caused by the presence of excluded volume. α is not an independent parameter because at equilibrium the

second-moment equation, eq 42, reduces to the following consistency relationship between z, μ, and α,

$$z = (1 - \alpha^{-2})[\alpha^2 + \mu^2]^{5/2} \tag{46}$$

The well-known scaling relation for the end-to-end distance with the number of monomers N, namely, $\sqrt{\langle Q^2\rangle_{eq}} \propto N^{3/5}$, may be obtained from eqs 45 and 46 in the limit of large N by noting that, because excluded volume is a pairwise interaction, z must scale as $\sqrt{N}$ for dumbbells.[10]

Substituting the expansion, eq 44, into the evolution equation, eq 42, leads to

$$\frac{d}{dt^*}\epsilon = \kappa^* + \kappa^{*T} - \frac{1}{\tau^*}\epsilon \tag{47}$$

where

$$\tau^* = \left[1 - \frac{z\mu^2}{(\alpha^2 + \mu^2)^{7/2}}\right]^{-1} \tag{48}$$

Furthermore, the stress tensor, eq 43, up to first order in the velocity gradient (without the rheologically unimportant isotropic contribution) is given by

$$\frac{\boldsymbol{\tau}^p}{nk_BT} = -H\epsilon \tag{49}$$

where

$$H = \alpha^2(\tau^*)^{-1} \tag{50}$$

Upon the integration of eq 47, which is a first-order ordinary differential equation for ϵ, and the substitution of the result into eq 49, the following codeformational integral expansion is obtained,

$$\boldsymbol{\tau}^p(t) = -\int_{-\infty}^{t} ds\, nk_BT\, \tilde{G}(t-s)\boldsymbol{\gamma}_{[1]}(t, s) \tag{51}$$

where $\boldsymbol{\gamma}_{[1]}$ is the codeformational rate-of-strain tensor[4] and the memory function $\tilde{G}(t)$ is given by

$$\tilde{G}(t) = H\, e^{-(t/\lambda_H\tau^*)} \tag{52}$$

The product $\lambda_H\tau^*$ is usually interpreted as a relaxation time and H as a relaxation weight. Clearly, the incorporation of excluded-volume effects increases the relaxation time in a good solvent relative to a θ-solvent by a factor of τ^*.

The memory function $\tilde{G}(t)$ can now be used to derive the linear viscoelastic material properties. Substituting $G(t) = nk_BT\tilde{G}(t)$ into eq 15 leads to

$$\frac{\eta'(\omega)}{\lambda_H nk_BT} = \frac{\tau^*H}{1 + (\lambda_H\tau^*\omega)^2}, \quad \frac{\eta''(\omega)}{\lambda_H^2 nk_BT} = \frac{\omega\tau^{*2}H}{1 + (\lambda_H\tau^*\omega)^2} \tag{53}$$

Upon taking the limit of $\omega \to 0$, we obtain,

$$\frac{\eta_{p,0}}{\lambda_H nk_BT} = \tau^*H, \quad \frac{\Psi_{1,0}}{\lambda_H^2 nk_BT} = 2\tau^{*2}H \tag{54}$$

At moderate-to-large values of the shear rate, it is not possible to obtain analytical expressions for the shear rate dependence of the viscometric functions, and consequently, a numerical procedure is required. Because the second moment $\langle \mathbf{Q}^*\mathbf{Q}^*\rangle$ shares the symmetry of the flow field in simple shear flow, its Cartesian components can be denoted by

$$\langle \mathbf{Q}^*\mathbf{Q}^*\rangle = \begin{pmatrix} s_1 & s_4 & 0 \\ s_4 & s_2 & 0 \\ 0 & 0 & s_3 \end{pmatrix} \tag{55}$$

When eq 55 is substituted into eq 42, a system of four first-order ordinary differential equations for the quantities s_j, $j = 1-4$, is obtained. Steady-state viscometric functions, as functions of shear rate, can then be found by numerically integrating these equations with respect to time (using a simple Euler scheme) until steady state is reached. Results obtained by this procedure are discussed in section 7.

5.4. First-Order Perturbation Expansion in *z*. The influence of excluded-volume effects on the universal shear rate dependence of viscometric functions has been studied, as mentioned earlier, by using renormalization group methods.[14,23] The renormalization group theory approach is essentially a method for refining the results of a low-order perturbation expansion in z, by introducing higher-order interaction effects so as to remove the ambiguous definition of the bead size. Results of this approach, based on a δ-function excluded-volume potential, indicate that the presence of excluded volume has a nontrivial influence on the shear rate dependence of the viscometric functions. We have seen earlier in this work that as far as equilibrium swelling and zero shear rate properties are concerned, the use of a δ-function excluded-volume potential leads to trivial results. In this section, a first-order perturbation expansion in z, with a narrow Gaussian excluded-volume potential, is constructed to compare its predictions of shear rate dependence with those obtained with Brownian dynamics simulations and with the Gaussian approximation. The dependence of the predictions on the width parameter μ is of particular interest.

A first-order perturbation expansion can be constructed, following the procedure suggested earlier[13,14] from the second-moment equation, eq 8. We assume that the configurational distribution function ψ can be written as $\psi_\theta + \psi_z$, where ψ_θ is the distribution function in the absence of excluded volume, i.e., in a θ-solvent, and ψ_z is the correction to first order in the strength of the excluded-volume interaction. The averages performed with these contributions will be denoted by $\langle\cdots\rangle_\theta$ and $\langle\cdots\rangle_z$, respectively.

When terms of equal order are equated, eq 8 can be rewritten as two equations, namely, a zeroth-order second-moment equation and a first-order second-moment equation. The zeroth-order equation, which is linear in the moment $\langle \mathbf{Q}^*\mathbf{Q}^*\rangle_\theta$, is the well-known second-moment equation for Hookean dumbbells in a θ-solvent.[5] It has the analytical solution[5]

$$\langle \mathbf{Q}^*\mathbf{Q}^*\rangle_\theta = \mathbf{1} - \int_{-\infty}^{t^*} ds^*\, e^{-(t^*-s^*)}\boldsymbol{\gamma}_{[0]}(t^*, s^*) \tag{56}$$

where $\boldsymbol{\gamma}_{[0]}$ is the codeformational relative strain tensor.[4] The first-order second-moment equation has the form

$$\frac{d}{dt^*}\langle \mathbf{Q}^*\mathbf{Q}^*\rangle_z = \kappa^*\cdot\langle \mathbf{Q}^*\mathbf{Q}^*\rangle_z + \langle \mathbf{Q}^*\mathbf{Q}^*\rangle_z\cdot\kappa^{*T} - \langle \mathbf{Q}^*\mathbf{Q}^*\rangle_z + \frac{z}{\mu^5}\langle e^{-(Q^{*2}/2\mu^2)}\mathbf{Q}^*\mathbf{Q}^*\rangle_\theta \tag{57}$$

The θ-solvent distribution function ψ_θ is a Gaussian,[5] and consequently, the complex moment on the right-hand side of eq 57 can be reduced to a function of $\langle \mathbf{Q}^*\mathbf{Q}^* \rangle_\theta$. The following equation is obtained on performing this reduction,

$$\frac{\mathrm{d}}{\mathrm{d}t^*}\langle \mathbf{Q}^*\mathbf{Q}^* \rangle_z = \boldsymbol{\kappa}^*\cdot\langle \mathbf{Q}^*\mathbf{Q}^* \rangle_z + \langle \mathbf{Q}^*\mathbf{Q}^* \rangle_z\cdot\boldsymbol{\kappa}^{*T} - \langle \mathbf{Q}^*\mathbf{Q}^* \rangle_z + \mathbf{Y} \quad (58)$$

where

$$\mathbf{Y} = \frac{z}{\sqrt{\det[\langle \mathbf{Q}^*\mathbf{Q}^* \rangle_\theta + \mu^2\,\mathbf{1}]}}[\langle \mathbf{Q}^*\mathbf{Q}^* \rangle_\theta + \mu^2\,\mathbf{1}]^{-1}\cdot\langle \mathbf{Q}^*\mathbf{Q}^* \rangle_\theta$$

Clearly, eq 58 also could have been derived by expanding the second-moment equation for the Gaussian approximation, eq 42, to first order in z. It follows, therefore, that the Gaussian approximation is exact to first order in z. This is also the situation in the case of the Gaussian approximation introduced for the treatment of hydrodynamic-interaction effects, where it was found to be exact to first order in the strength of hydrodynamic interaction, h^*.[13]

Equation 58 is a system of linear inhomogeneous ordinary differential equations whose solution is

$$\langle \mathbf{Q}^*\mathbf{Q}^* \rangle_z = \int_{-\infty}^{t^*} \mathrm{d}s^*\, e^{-(t^*-s^*)}\mathbf{E}(t^*, s^*)\cdot\mathbf{Y}\cdot\mathbf{E}^T(t^*, s^*) \quad (59)$$

where $\mathbf{E}$ is the displacement gradient tensor.[4]

The expression for the stress tensor, eq 7, can also be expanded to first order in z. After reduction of complex moments to second moments, the stress tensor depends only on the second moments $\langle \mathbf{Q}^*\mathbf{Q}^* \rangle_\theta$ and $\langle \mathbf{Q}^*\mathbf{Q}^* \rangle_z$. Equations 56 and 59 may then be used to derive the following first-order perturbation theory expression for the stress tensor in arbitrary homogeneous flows,

$$\frac{\boldsymbol{\tau}^{\mathrm{p}}}{nk_{\mathrm{B}}T} = \mathbf{Y} + \int_{-\infty}^{t^*} \mathrm{d}s^*\, e^{-(t^*-s^*)}\{\boldsymbol{\gamma}_{[0]}(t^*, s^*) - \mathbf{E}(t^*, s^*)\cdot\mathbf{Y}\cdot\mathbf{E}^T(t^*, s^*)\} \quad (60)$$

Note that $\mathbf{Y}$, the direct contribution to the stress tensor, is isotropic only in the limit $\mu \to 0$.

The form in steady shear flow of the tensors $\boldsymbol{\gamma}_{[0]}$ and $\mathbf{E}$ has been tabulated previously.[4] By use of the expression for the stress tensor, eq 60, and the definition of the viscometric functions, eq 11, the following first-order perturbation theory results for the viscometric functions are obtained,

$$\frac{\eta_{\mathrm{p}}}{\lambda_H nk_{\mathrm{B}}T} = 1 + \left(\frac{1 + \mu^2 + \lambda_H^2\dot{\gamma}^2}{\sqrt{1+\mu^2}\,\Delta^{3/2}}\right)z \quad (61)$$

$$\frac{\Psi_1}{\lambda_H^2 nk_{\mathrm{B}}T} = 2 + 2\left(\frac{1 + 2\mu^2 + \lambda_H^2\dot{\gamma}^2}{\sqrt{1+\mu^2}\,\Delta^{3/2}}\right)z \quad (62)$$

where $\Delta = (1+\mu^2)[1 + \mu^2 + 2\lambda_H^2\dot{\gamma}^2] - \lambda_H^2\dot{\gamma}^2$. In the limit of $\lambda_H\dot{\gamma}$ going to zero, the expression for the viscosity, eq 61, reduces to the expression derived earlier in section 5.1, using the retarded-motion expansion and the equilibrium perturbation expansion, for the zero shear rate viscosity. One can also show that $\mathrm{tr}\langle \mathbf{Q}^*\mathbf{Q}^* \rangle$ reduces to the equilibrium moment q_1 (see eq 38), in the limit $\lambda_H\dot{\gamma} \to 0$.

The first-order perturbation results are compared with simulation results and with results of the Guassian approximation in section 7.

6. Fixman's Theory

Many years ago, in path-breaking seminal work, Fixman[9] considered the simultaneous inclusion of hydrodynamic interaction and excluded volume in bead−spring chain models for dilute polymer solutions. To render the problem solvable, Fixman introduced a number of approximations. Because we are only concerned with excluded volume in the context of Hookean dumbbells in this work, we shall consider only those approximations which are relevant in this context. The introduction of the quadratic potential, the governing equations of Fixman's theory, and the calculation of material functions predicted by the theory in simple shear flow are considered in this section.

6.1. The Quadratic Potential. With regard to excluded volume, the most crucial approximation of Fixman[9] is the replacement of the δ-function potential with a quadratic potential. By adopting a Boson operator formulation of the governing equations, Fixman has shown that the δ-function potential, eq 27, may be represented by

$$E^*(\mathbf{Q}^*) = \frac{1}{2}\mathbf{Q}^*\cdot\mathbf{G}^*\cdot\mathbf{Q}^* \quad (63)$$

where $\mathbf{G}^*$ is a symmetric function of various configuration-dependent quantities introduced in the Boson operator formalism. From this expression, it is clear that a quadratic potential for the excluded volume may be obtained by replacing the fluctuating quantity $\mathbf{G}^*$ with an average. Fixman obtains a quadratic potential by replacing $\mathbf{G}^*$ with a configuration-dependent average, as described below.

As a result of replacing $\mathbf{G}^*$ with its average, one can show from eq 63 that

$$\langle \mathbf{G}^* \rangle = \left\langle \frac{\partial}{\partial \mathbf{Q}^*}\frac{\partial E^*}{\partial \mathbf{Q}^*} \right\rangle \quad (64)$$

In other words, for any given potential E^*, one can find $\langle \mathbf{G}^* \rangle$ provided that the nonequilibrium distribution function $\psi(\mathbf{Q}, t)$ with which to carry out the average on the right-hand side of eq 64 is known. It turns out that $\psi(\mathbf{Q}, t)$, in the presence of a quadratic excluded-volume potential and with consistently averaged hydrodynamic interaction,[12,16] is a Gaussian distribution. Evaluation of the average for a δ-potential, eq 27, with a Gaussian distribution, eq 41, leads to the following nondimensional quadratic potential,

$$E^*(\mathbf{Q}^*) = -\frac{1}{2}\frac{z}{\sqrt{\det\langle \mathbf{Q}^*\mathbf{Q}^* \rangle}}\mathbf{Q}^*\cdot\langle \mathbf{Q}^*\mathbf{Q}^* \rangle^{-1}\cdot\mathbf{Q}^* \quad (65)$$

It is straightforward to show that the potential, eq 65, leads to an unphysical *noncentral* excluded-volume force between the beads. Fixman, perhaps for this reason, introduces a further approximation which consists of

replacing the above potential with the following simpler form,

$$E^*(\mathbf{Q}^*) = -\frac{1}{2}\frac{z}{\alpha^2}\frac{Q^{*2}}{\sqrt{\det\langle\mathbf{Q}^*\mathbf{Q}^*\rangle}} \tag{66}$$

where α is defined as before by eq 45. However, in this case, α obeys the consistency relation,

$$z = (\alpha^2 - 1)\alpha^3 \tag{67}$$

Interestingly enough, eq 46 reduces to eq 67 in the limit $\mu \to 0$ (which corresponds to a δ-potential).

It is appropriate here to note that while Fixman has presented all his arguments for bead−spring chain models, the form of Fixman's potential for dumbbells given above can be found in the book by Larson.[10]

The consequences of adopting the quadratic excluded-volume potential, eq 66, are briefly discussed in the following section. It is worthwhile to point out here that Fixman's original formulation of the problem was not in terms of the Gaussian distributions and second moments discussed below. Rather, his attempt was to directly solve the diffusion equation, eq 1, for the configurational distribution function, and then carry out the average in eq 2 to obtain the rheological properties. It is, however, possible to discuss his approach within the framework developed subsequently by Öttinger,[12] and this is the procedure that is adopted here. A graphic exposition of Fixman's algorithm is given elsewhere.[10]

6.2. The Governing Equations. With excluded-volume interactions described by the quadratic potential, eq 66, the diffusion equation, eq 1, becomes linear in the bead-connector vector. As a result, the diffusion equation is exactly satisfied by a Gaussian distribution, eq 41. In Fixman's theory, therefore, a tractable model is obtained not by approximating the distribution function, as in the case of the Gaussian approximation, but by introducing the quadratic potential, eq 66.

Although $\psi(\mathbf{Q}, t)$ is a Gaussian both in the Gaussian approximation and in Fixman's theory, the second moment which completely determines these distributions is different in the two cases. In Fixman's theory, the nondimensional second moment $\langle\mathbf{Q}^*\mathbf{Q}^*\rangle$ is governed by the equation

$$\frac{\mathrm{d}}{\mathrm{d}t^*}\langle\mathbf{Q}^*\mathbf{Q}^*\rangle = \boldsymbol{\kappa}^*\cdot\langle\mathbf{Q}^*\mathbf{Q}^*\rangle + \langle\mathbf{Q}^*\mathbf{Q}^*\rangle\cdot\boldsymbol{\kappa}^{*T} - \left[1 - \frac{z}{\alpha^2\sqrt{\det\langle\mathbf{Q}^*\mathbf{Q}^*\rangle}}\right]\langle\mathbf{Q}^*\mathbf{Q}^*\rangle + \mathbf{1} \tag{68}$$

Note that the second-moment equation reduces to eq 67 at equilibrium.

The Giesekus expression for the stress tensor has the form

$$\frac{\boldsymbol{\tau}^p}{nk_BT} = -\left[1 - \frac{z}{\alpha^2\sqrt{\det\langle\mathbf{Q}^*\mathbf{Q}^*\rangle}}\right]\langle\mathbf{Q}^*\mathbf{Q}^*\rangle + \mathbf{1} \tag{69}$$

As a result, the stress tensor in Fixman's theory, for any flow situation, may be obtained once eq 68 is solved for $\langle\mathbf{Q}^*\mathbf{Q}^*\rangle$.

It is clear from eq 69 that in Fixman's theory, as for $\mu > 0$ in the Gaussian approximation, rheological properties are affected both directly and indirectly by the presence of excluded volume.

As will be shown in the section below, at *steady state* in simple shear flow, the problem of solving the governing equation for the second moments, eq 68, reduces to one of solving a single nonlinear algebraic equation. In the linear viscoelastic limit, however, analytical expressions for the various properties can be derived in the same manner as described earlier for the Gaussian approximation. Indeed, it can be shown that the linear viscoelastic properties are given by eqs 53 and 54, where the quantities H and τ^* are now given by

$$H = 1, \quad \tau^* = \alpha^2 \tag{70}$$

In steady simple shear flow, substituting eq 55 for $\langle\mathbf{Q}^*\mathbf{Q}^*\rangle$ and eq 10 for κ into the second-moment equation, eq 68, leads to the following equations for the components of $\langle\mathbf{Q}^*\mathbf{Q}^*\rangle$,

$$s_1 = (1 + 2\lambda_H^2\dot\gamma^2 s_2^2)s_2, \quad s_3 = s_2, \quad s_4 = \lambda_H\dot\gamma s_2^2$$

where s_2 must satisfy the nonlinear algebraic equation

$$s_2^{3/2} - s_2^{1/2} = \frac{\alpha(\alpha^2 - 1)}{\sqrt{1 + \lambda_H^2\dot\gamma^2 s_2^2}} \tag{71}$$

The normalized viscometric functions can be found by using the definitions in eq 11 and the results above for the zero shear rate properties,

$$\frac{\eta_p}{\eta_{p,0}} = \frac{s_2}{\alpha^2}, \quad \frac{\Psi_1}{\Psi_{1,0}} = \frac{s_2^2}{\alpha^4}, \quad \Psi_2 = 0 \tag{72}$$

The nonlinear algebraic equation, eq 71, is solved here with a Newton−Raphson scheme. The material functions predicted by Fixman's theory are compared with the predictions of the narrow Gaussian potential in the section below.

7. Results and Discussion

The predictions of rheological properties in simple shear flow, by the various theories for the excluded-volume effect, are compared in this section. Predictions in the limit of zero shear rate are first considered below, and those at finite nonzero shear rates subsequently.

7.1. Zero Shear Rate Properties. Figure 1 is a plot of $(\eta_{p,0}/\lambda_H nk_BT)$ versus μ for $z = 3$ and 100. The continuous curves are exact predictions obtained by numerical quadrature, and the triangles and circles are exact results of Brownian dynamics simulations carried out at equilibrium (without variance reduction) (see eq 31). The dashed lines are the predictions of the Gaussian approximation for the narrow Gaussian potential (i.e., eq 54, with τ^* and H given by eqs 48 and 50, respectively), the dot−dashed curve is the prediction of the first-order perturbation theory (i.e., eq 61 in the limit $\lambda_H\dot\gamma \to 0$), and the filled squares are the predictions of Fixman's theory (i.e., eq 54, with τ^* and H given by eq 70). The parameter μ does not enter into Fixman's theory; however, these values are plotted corresponding to $\mu = 0$, because the quadratic potential is used in Fixman's theory as an approximation for the δ-potential.

The first feature to be noticed in Figure 1 is the reassuring closeness of the exact results obtained by using the retarded-motion expansion and by Brownian dynamics simulations. The retarded-motion expansion

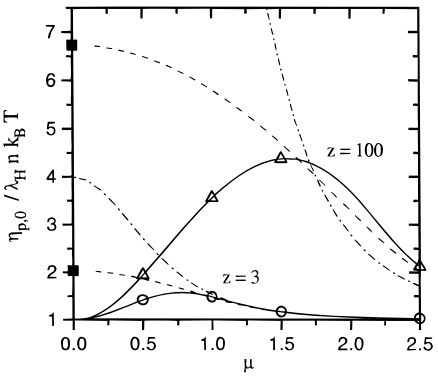

Figure 1. Nondimensional zero shear rate viscosity versus the extent of excluded-volume interaction μ, for two values of the strength of the interaction z. The continuous lines are exact predictions obtained by numerical quadrature, the triangles and circles are results of Brownian dynamics simulations, the dashed and the dot−dashed lines are the approximate predictions of the Gaussian approximation, and the first-order perturbation theory, respectively, and the filled squares are the predictions of Fixman's theory. The error bars in the Brownian dynamics simulations cannot be resolved within the line thickness.

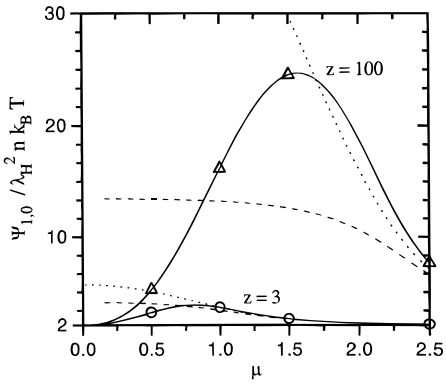

Figure 2. Nondimensional zero shear rate first normal stress difference versus μ, for two values of z. The continuous lines are exact predictions obtained by numerical quadrature, the triangles and circles are results of Brownian dynamics simulations, the dashed lines are approximate predictions using the Gaussian approximation, and the dotted lines are approximate predictions using the uniform-expansion model. The error bars in the Brownian dynamics simulations cannot be resolved within the line thickness.

provides a means of validating the results of Brownian dynamics simulations.

In the limit $\mu \to 0$ and for large values of μ, the continuous curves and Brownian dynamics simulations reveal that, as expected, the exact predictions of the narrow Gaussian potential tend to the z-independent θ-solvent value, $(\eta_{p,0}/\lambda_H n k_B T) = 1$. This implies, as pointed out earlier, that the use of a δ-function potential to represent excluded-volume interactions does not lead to any change in the zero shear rate viscosity prediction. On the other hand, Figure 1 seems to suggest that a finite range of excluded-volume interaction is required to cause a change from the θ-solvent value. Away from these limits, at nonzero values of μ, the narrow Gaussian potential predicts an increase in the value of zero shear rate viscosity. The existence of shear thinning in good solvents can be attributed to this increase. This follows from the fact that at high shear rates, as the effect of the excluded-volume interaction diminishes, the viscosity is expected to return to its θ-solvent value. We shall see later that this expectation is indeed justified.

The dashed lines in Figure 1 indicate that in the limit of zero shear rate, for a given value of z, the Gaussian approximation is reasonably accurate above a certain value of μ. This limiting value of μ appears to be smaller for smaller values of z. A similar behavior is also observed with regard to the prediction of the zero shear rate first normal stress difference (see Figure 2). Thus, it appears that the exact configurational distribution function $\psi(\mathbf{Q}, t)$ becomes increasingly non-Gaussian as the narrow Gaussian potential becomes narrower and the strength of the excluded-volume interaction becomes larger.

For the large values of z considered in Figure 1, results obtained with the first-order perturbation expansion in z cannot be expected to be accurate. It is clear from the dot−dashed lines that the perturbation expansion results deviate significantly from exact results for small values of μ. However, they become increasingly accurate as μ increases, for a given value of z. This can be understood by considering eq 61, which indicates that in the limit $\lambda_H \dot{\gamma} \to 0$, the first-order correction to the θ-solvent value increases as z increases but decreases as μ increases.

As μ increases from zero, values of the zero shear rate viscosity predicted by the Gaussian approximation approach the exact values more rapidly than the predictions of the first-order perturbation theory, for a given value of z. The Gaussian approximation is a nonperturbative approximation; however, it was shown in section 5.4 to be exact to first order in z. One way to understand this is to consider the Gaussian approximation to consist of an infinite number of higher-order terms, whose nature is unknown. In this sense, it is an *uncontrolled* approximation, which remains accurate at values of z and μ, where the first-order perturbation expansion becomes inaccurate. As will be seen shortly, these remarks also apply to the results obtained at finite shear rate.

The difference in the prediction of the zero shear rate viscosity by Fixman's theory and that by the narrow Gaussian potential is evident in Figure 1. It is also worth noting that, although the relaxation weight and the relaxation time are different in Fixman's theory and in the Gaussian approximation for $\mu = 0$, they lead to the same prediction of the zero shear rate viscosity. This is, however, not true for the zero shear rate first normal stress difference. The ratio $U_{\Psi\eta}$, defined by[15]

$$U_{\Psi\eta} = \frac{nk_B T\Psi_1}{\eta_p^2} \tag{73}$$

is equal, in the zero shear rate limit, to $(2/\alpha^2)$ in the Gaussian approximation, while it has a constant value of 2 in Fixman's theory.

Both the uniform-expansion model and the Gaussian approximation use Gaussian distributions in order to evaluate averages. However, the uniform-expansion model uses different Gaussian distributions for different equilibrium averages, such that the best approximation is obtained. Although this does not lead to any difference in the prediction of the zero shear rate viscosity by the two approximations, Figure 2 reveals that at small-enough values of μ there is a significant difference in the prediction of the zero shear rate first normal stress difference. Clearly, the uniform-expansion model continues to be a reasonable approximation for values of μ at which the Gaussian approximation is no longer

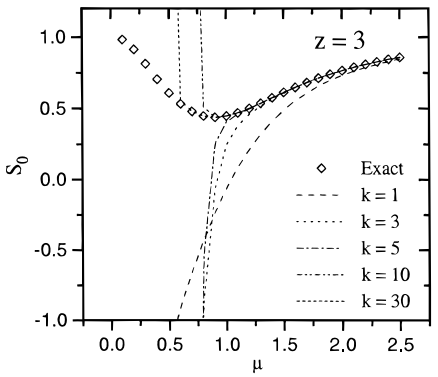

Figure 3. S_0 versus μ for different numbers of summed terms k in the perturbation expansion (see eq 37). The exact results are obtained by numerical quadrature.

accurate. However, even the uniform-expansion model leads to a poor approximation at sufficiently small values of μ.

In the discussion of the equilibrium perturbation expansion in section 5.1.2, it was pointed out that in principle the equilibrium moment q_1 can be obtained for any nonzero value of μ, provided that enough numbers of terms in the series for the quantities S_0 and S_1, are summed (see eq 37). Figure 3 displays the sum S_0 for different numbers of summed terms in the perturbation expansion, as a function of μ, for $z = 3.0$. Exact results are obtained by noting that $S_0 = \sqrt{2/\pi} I_0$ and evaluating I_0 by numerical quadrature. Clearly, more terms of the expansion are required for convergence as μ decreases. The terms of the series, which are alternating in sign, keep increasing rapidly in magnitude, until $n \gtrsim z/\mu^3$, before they begin to decrease. Therefore, as z increases, or as μ decreases, more and more terms are required for the sum to converge. Above a threshold value of z/μ^3 however, it becomes impossible to evaluate S_0 because the round-off errors due to the summation of large numbers makes the perturbation expansion numerically useless. A similar problem is also encountered while evaluating S_1. In short, the hope of extrapolating finite μ results to the limit $\mu = 0$, cannot be realized. Therefore, in the case of Hookean dumbbells, one cannot obtain equilibrium moments for a δ-function excluded-volume potential by using a narrow Gaussian potential and considering a perturbation expansion in the limit $\mu \to 0$.

7.2. Steady-State Viscometric Functions. The results of Brownian dynamics simulations (without variance reduction) displayed in Figure 4 reveal that the dependence of the viscosity and the first normal stress difference on μ, at a value of the nondimensional shear rate $\lambda_H\dot{\gamma} = 0.3$, is similar in shape to the dependence observed in the limit of zero shear rate. At small and large values of μ, the material functions tend to the θ-solvent value and exhibit a maximum at some value in between. Because, even at this nonzero value of shear rate, it appears that the viscosity and the first normal stress difference remain at their θ-solvent values for $\mu = 0$, it implies that the use of a δ-potential to represent excluded-volume interactions would not predict any shear thinning. On the other hand, as we shall see subsequently, a quadratic potential does predict substantial shear thinning. At $\lambda_H\dot{\gamma} = 0.3$, the Gaussian approximation seems to be accurate above roughly the same values of μ as were observed in the limit of zero shear rate.

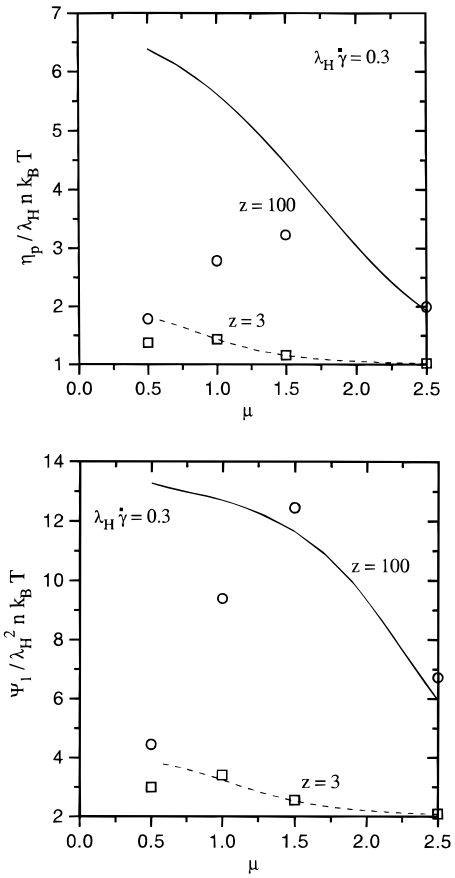

Figure 4. Nondimensional viscosity and first normal stress difference versus μ for two values of z, at a nondimensional shear rate $\lambda_H\dot{\gamma} = 0.3$. The squares and circles are results of Brownian dynamics simulations, and the dashed and continuous lines are the predictions of the Gaussian approximation, for $z = 3$ and 100, respectively. The error bars in the Brownian dynamics simulations cannot be resolved within the line thickness.

Figures 5 and 6 are plots of nondimensional viscosity and first normal stress difference versus the nondimensional shear rate $\lambda_H\dot{\gamma}$. Figure 5 displays the dependence of these viscometric functions on the parameter μ for a fixed value of $z = 0.1$, and Figure 6 displays the dependence on the parameter z for a fixed value of $\mu = 2.5$. The prediction of shear thinning for nonzero values of μ is apparent, and our earlier expectation in this direction is justified. In particular, the predictions of Brownian dynamics simulations, the Gaussian approximation, and the first-order perturbation theory tend to θ-solvent values at high shear rates.

Shear thinning, which is seemingly physically meaningful, is also predicted, as can be seen from Figure 5, by both the Gaussian approximation and the first-order perturbation theory, for $\mu = 0$. This corresponds to a δ-function excluded-volume potential and is clearly an artifact of the perturbation expansion, because rigorous calculations indicate a trivial result. It remains to be seen if the situation is different in the limit of long chains.

For small-enough values of z and large-enough values of μ, the results of the Gaussian approximation and the first-order perturbation expansion agree exceedingly well with the exact results of Brownian dynamics simulations. Indeed, as $\lambda_H\dot{\gamma}$ increases for fixed values of z and μ, both the Gaussian approximation and the first-order perturbation expansion become increasingly

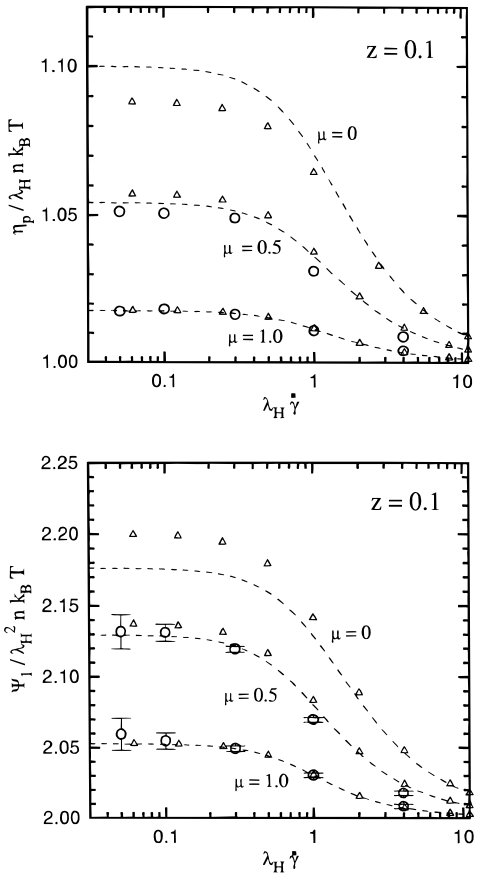

Figure 5. Nondimensional viscosity and first normal stress difference versus nondimensional shear rate $\lambda_H\dot{\gamma}$, for three values of μ at $z = 0.1$. The circles are results of Brownian dynamics simulations, the dashed lines are the predictions of the Gaussian approximation, and the triangles are the predictions of the first-order perturbation expansion. In the viscosity plot, the error bars in the Brownian dynamics simulations are smaller than the size of the symbols.

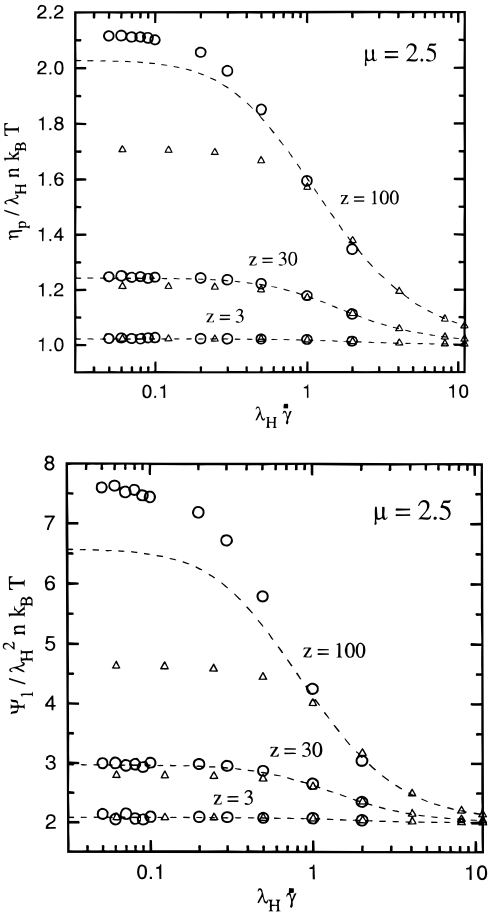

Figure 6. Nondimensional viscosity and first normal stress difference versus $\lambda_H\dot{\gamma}$ for three values of z, at $\mu = 2.5$. The symbols are as indicated in the caption to Figures 5. The error bars in the Brownian dynamics simulations are smaller than the size of the symbols.

accurate. In particular, if both of the approximations are accurate at zero shear rate, they continue to remain accurate at nonzero shear rates. This can be understood in the case of the first-order perturbation expansion by considering eqs 61 and 62. Clearly, the departure from the θ-solvent values decreases as $\lambda_H\dot{\gamma}$ increases. This is in line with the intuitive expectation of decreasing excluded-volume interactions with increasing shear rate.

For a fixed value of the shear rate $\lambda_H\dot{\gamma}$, as z increases or μ decreases, the predictions of the Gaussian approximation and the first-order perturbation expansion become increasingly inaccurate, with the first-order perturbation expansion breaking down before the Gaussian approximation. This can be expected, because the Gaussian approximation, being exact to first order in z, is at least as accurate as the first-order perturbation expansion.

The two different Brownian dynamics simulation algorithms mentioned in section 5.2 were used to obtain the data in Figures 5 and 6. While the algorithm with variance reduction was used for shear rates up to $\lambda_H\dot{\gamma} = 0.1$, the algorithm without variance reduction was used at higher shear rates. With regard to the results obtained by variance reduction, it was found that the variance was typically reduced by a factor of 5 to 10 by the parallel equilibrium simulation subtraction procedure. While the magnitude of the reduced variance was relatively independent of shear rate for the viscosity, it decreased with increasing shear rate for the first normal stress difference. The time to reach steady state, from start-up of flow, was roughly 10 relaxation times for $z = 0.1$, 3, and 30 and roughly 15 relaxation times for $z = 100$. Rheological properties in the two parallel simulations remained correlated during the time required to reach steady state, and as a result, the present technique proved adequate for the purpose of variance reduction.

We have seen earlier (Figure 1) that both Fixman's theory and the Gaussian approximation for $\mu = 0$ lead to identical values for the zero shear rate viscosity. This coincidence is, however, restricted to the limit of zero shear rate. At nonzero shear rates, as can be seen from Figure 7, there is considerable divergence between the predictions of the two theories.

Fixman's theory for dumbbells, though differing considerably from the narrow Gaussian potential in terms of its predictions of rheological properties, has the appealing aspect that it captures some of the *universal* features of the behavior of good solvents, which can only be expected from bead−spring chain theories in the limit of a large number of beads. We have seen this universal behavior earlier in the correct prediction of the end-to-end distance scaling and in the parameter-free nature of the ratio $U\Psi_\eta$. Figure 8 displays the prediction by Fixman's theory of the reduced variable $\eta_p/\eta_{p,0}$ versus the nondimensional shear rate $\beta = \lambda_p\dot{\gamma}$, where $\lambda_p =$

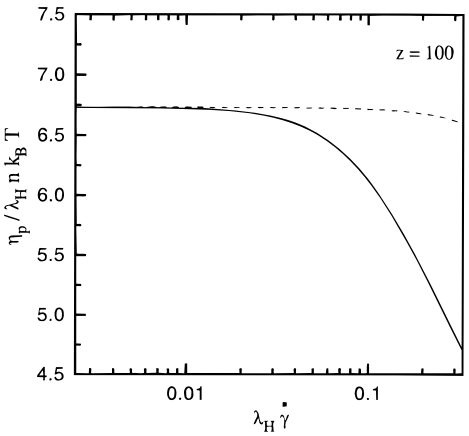

Figure 7. Nondimensional viscosity versus nondimensional shear rate for $z = 100$. The continuous line is the prediction of Fixman's theory, and the dashed line is the prediction of the Gaussian approximation for $\mu = 0$.

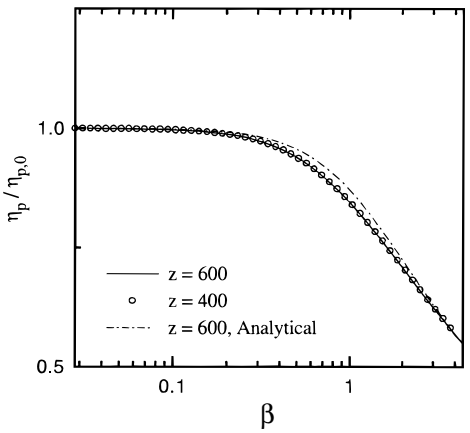

Figure 8. Reduced viscosity versus reduced shear rate predicted by Fixman's theory for large values of z. The continuous line and circles are obtained numerically, while the dot−dashed line is obtained with the analytical expression, eq 74.

$[\eta]_0 M \eta_s / N_A k_B T$, is a characteristic relaxation time. Here, $[\eta]_0$ is the zero shear rate intrinsic viscosity, M is the molecular weight, and N_A is Avogadro's number. For dilute solutions, one can show that $\beta = \eta_{p,0}\dot{\gamma}/nk_BT$. The figure clearly reveals that as $z \rightarrow \infty$ the curves for different values of z overlap. Therefore, in this respect also, Fixman's theory mimics the universal behavior expected of long chains. The source of this behavior can be understood by examining eq 71. In the limit of $\alpha \gg 1$, one can show that $s_2 = [\alpha^6(\lambda_H\dot{\gamma})^{-2}]^{1/5}$. As a result, $\eta_p/\eta_{p,0} = [\alpha^2\lambda_H\dot{\gamma}]^{-2/5}$, leading to the observed scaling. At small values of $\lambda_H\dot{\gamma}$, $\eta_p/\eta_{p,0} \rightarrow 1$. One can therefore construct the analytical expression

$$\frac{\eta_p}{\eta_{p,0}} = (1 + \alpha^4\lambda_H^2\dot{\gamma}^2)^{-1/5} \tag{74}$$

and expect it to be accurate at very small and large values of β. The dot−dashed curve in Figure 8 shows that eq 74 is accurate over a fairly wide range of β.

The universal behavior discussed above is not exhibited by the Gaussian approximation. The reason for this can be easily understood in the limit $\mu \rightarrow 0$, where the second-moment equation, eq 42, reduces at steady state to a nonlinear algebraic equation. Indeed, one can show that for $\alpha \gg 1$, $\eta_p/\eta_{p,0} = [1 + \lambda_H^2\dot{\gamma}^2]^{-1/5}$. As a result, the

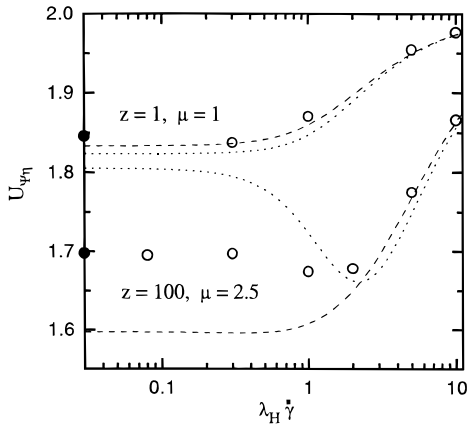

Figure 9. The ratio $U_{\Psi\eta}$ (see eq 73) versus $\lambda_H\dot{\gamma}$. The circles are results of Brownian dynamics simulations, the dashed lines are the predictions of the Gaussian approximation, and the dotted lines are the predictions of the first-order perturbation expansion. The filled circles on the y-axis represent zero shear rate values of $U_{\Psi\eta}$ obtained by equilibrium simulations. The error bars in the Brownian dynamics simulations are smaller than the size of the symbols.

normalized material functions do not collapse onto a single curve when plotted versus β. It is, however, not realistic to expect a dumbbell model to exhibit universal features, and the real verification of universal behavior requires the development of a theory for long bead−spring chains.

The nondimensional ratio $U_{\Psi\eta}$ (see eq 73) has a constant value of 2, independent of shear rate, for Hookean dumbbells in θ-solvents and in Fixman's theory for good solvents. Figure 9 displays the predictions of $U_{\Psi\eta}$ for the narrow Gaussian potential, obtained by the Brownian dynamics simulations, the Gaussian approximation, and the following first-order perturbation expansion (which can be derived from eqs 61 and 62),

$$U_{\Psi\eta} = 2 - 2z\frac{1 + \lambda_H^2\dot{\gamma}^2}{\sqrt{1 + \mu^2}\Delta^{3/2}} \tag{75}$$

where Δ has been defined below eq 62. Because a logarithmic scale has been chosen for the shear rate axis, it is difficult to represent the zero shear rate value of $U_{\Psi\eta}$. However, because it is very nearly constant at low values of shear rate, the zero shear rate value is represented in Figure 9 by the filled circles on the y-axis. All of the data in Figure 9 have the same trend of remaining nearly constant at low shear rates and approaching asymptotically the value of 2 at high shear rates. In the case of the first-order perturbation expansion, this can be understood by considering eq 75 in the limit $\lambda_H\dot{\gamma} \rightarrow \infty$.

The dependence of the mean-squared end-to-end distance $\langle Q^{*2}\rangle$ on $\lambda_H\dot{\gamma}$ is revealed in Figure 10. The circles and triangles are the results of Brownian dynamics simulations obtained with the algorithm without variance reduction. The dotted and dashed lines are plots of the following expression,

$$\langle Q^{*2}\rangle = 3 + 2\lambda_H^2\dot{\gamma}^2 + \frac{z}{\sqrt{1 + \mu^2}\Delta^{3/2}}[3(1 + \mu^2) + (5 + 6\mu^2)\lambda_H^2\dot{\gamma}^2 + 2\lambda_H^4\dot{\gamma}^4]$$

obtained from the first-order perturbation expansion,

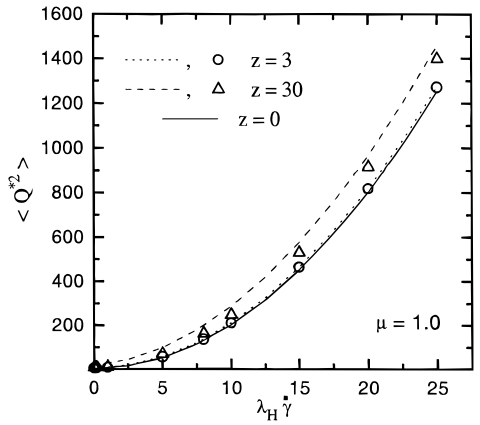

Figure 10. Dimensionless mean-squared end-to-end vector versus nondimensional shear rate $\lambda_H\dot{\gamma}$, for two values of z at $\mu = 1$. The circles and triangles are results of Brownian dynamics simulations, the dotted and dashed lines are the predictions of the first-order perturbation expansion, and the continuous line is the analytical solution for a θ-solvent. The error bars in the Brownian dynamics simulations are smaller than the size of the symbols.

and the continuous line is the well-known result for a θ-solvent,[5] $\langle Q^{*2}\rangle = 3 + 2\lambda_H^2\dot{\gamma}^2$. Interestingly, the effect of excluded-volume interactions on swelling increases with increasing shear rate. In the case of the first-order perturbation expansion, which appears to be accurate for $z = 3$ but not for $z = 30$, this can be understood by noting, in the expression above, that the term representing the correction to the θ-solvent result due to the presence of excluded volume increases as the shear rate increases.

8. Conclusions

The use of a narrow Gaussian potential to describe the excluded-volume interactions between the beads of a Hookean dumbbell model leads to the prediction of swelling and shear thinning for relatively small nonzero values of the extent of interaction μ. This is essentially caused by an increase in the magnitude of the equilibrium moments relative to their θ-solvent values. A δ-function description of the excluded-volume potential, on the other hand, is found to predict neither swelling nor shear thinning for Hookean dumbbells.

For a given strength of the excluded-volume interaction z, the Gaussian approximation is found to be reasonably accurate for values of μ larger than some threshold value. The behavior of the Gaussian approximation can be understood by comparing its predictions with those of a first-order perturbation expansion in z, because it is shown here to be exact to first order in z. The perturbation expansion reveals that the departure of the viscometric functions from their θ-solvent values increases with increasing z but decreases with increasing μ and increasing shear rate $\lambda_H\dot{\gamma}$.

The use of a quadratic potential in Fixman's theory leads to the prediction of viscometric functions which are considerably different from those of the narrow Gaussian potential. However, Fixman's theory for dumbbells reproduces a number of universal features observed in good solvents.

Acknowledgment. Support for this work through Grant III. 5(5)/98-ET from the Department of Science and Technology, India, to J. Ravi Prakash is acknowledged. Part of this work was carried out while J.R.P. was a participant in the research program *Jamming and Rheology* at the Institute for Theoretical Physics, University of California, Santa Barbara, CA. J.R.P. also thanks the nonlinear dynamics group at IIT Madras for providing the use of their computational facility.

A. The Uniform-Expansion Model

The equilibrium average of any quantity $X(\mathbf{Q})$ is given by

$$\langle X\rangle_{\mathrm{eq}} = N_{\mathrm{eq}} \int X(\mathbf{Q}) \exp\left\{-\frac{3}{2b^2}Q^2 - E^*\right\} \mathrm{d}\mathbf{Q} \tag{76}$$

where $b^2 = 3(k_BT/H)$. Through the multiplication and division of the integrand with the Gaussian distribution $\psi'_{\mathrm{eq}}(\mathbf{Q})$ (defined by eq 39) and the use of normalization conditions on $\psi_{\mathrm{eq}}(\mathbf{Q})$ and $\psi'_{\mathrm{eq}}(\mathbf{Q})$, eq 76 can be rewritten in the form

$$\langle X\rangle_{\mathrm{ep}} = \frac{\langle X(\mathbf{Q})\, e^{-B(\mathbf{Q})}\rangle'_{\mathrm{eq}}}{\langle e^{-B(\mathbf{Q})}\rangle'_{\mathrm{eq}}} \tag{77}$$

where $B(\mathbf{Q}) = (3/2)[(1/b^2) - (1/b'^2)]Q^2 + E^*$. For $\psi'_{\mathrm{eq}}(\mathbf{Q})$ to be a good approximation to $\psi_{\mathrm{eq}}(\mathbf{Q})$, $B(\mathbf{Q})$ must be small. On expanding $\exp[-B(\mathbf{Q})]$ in a Taylor's series, one can then write eq 77 to first order in $B(\mathbf{Q})$ as

$$\langle X\rangle_{\mathrm{eq}} = \langle X\rangle'_{\mathrm{eq}} - \langle XB\rangle'_{\mathrm{eq}} + \langle X\rangle'_{\mathrm{eq}}\langle B\rangle'_{\mathrm{eq}} \tag{78}$$

If b' is chosen such that $\langle XB\rangle'_{\mathrm{eq}} = \langle X\rangle'_{\mathrm{eq}}\langle B\rangle'_{\mathrm{eq}}$, it then follows that $\langle X\rangle_{\mathrm{eq}}$ is well-approximated by $\langle X\rangle'_{\mathrm{eq}}$.

The choice of b' that best optimizes the approximation clearly depends on the quantity $X(\mathbf{Q})$ that is averaged. In our case, we require averages of the quantities $X_{(m)} \equiv Q^{2m}$, where $m = 1-3$. From the well-known result for the moments of a Gaussian distribution,

$$\langle Q^{2m}\rangle'_{\mathrm{eq}} = \frac{2}{\sqrt{\pi}}\left[\frac{2b'^2_{(m)}}{3}\right]^m \Gamma\left(m + \frac{3}{2}\right) \tag{79}$$

where $b'_{(m)}$ represents the value of b' corresponding to Q^{2m}. It follows that the optimum value of $b'_{(m)}$ is found by solving the following nonlinear algebraic equation for $\alpha_{(m)}$,

$$(\alpha^2_{(m)} - 1)m + \frac{z}{[\alpha^2_{(m)} + \mu^2]^{3/2}}\left\{\frac{\mu^{2m}}{[\alpha^2_{(m)} + \mu^2]^m} - 1\right\} = 0 \tag{80}$$

where $\alpha_{(m)} = b'_{(m)}/b$, $m = 1-3$. In terms of $\alpha_{(m)}$,

$$u_m = \alpha^{2m}_{(m)} \prod_{p=1}^{m}(2p + 1) \tag{81}$$

References and Notes

(1) Ahn, K. H.; Lee, S. J. *J. Non-Newtonian Fluid Mech.* **1992**, *43*, 143. Ahn, K. H.; Schrag, J. L.; Lee, S. J. *J. Non-Newtonian Fluid Mech.* **1993**, *50*, 349.
(2) Andrews, N. C.; Doufas, A. K.; McHugh, A. J. *Macromolecules* **1998**, *31*, 3104.
(3) Arfken, G. *Mathematical Methods for Physicists*, 3rd ed.; Academic Press: Boston, 1985.
(4) Bird, R. B.; Armstrong, R. C.; Hassager, O. *Dynamics of Polymeric Liquids. Fluid Mechanics*, 2nd ed.; Wiley-Interscience: New York, 1987; Vol. 1.

(5) Bird, R. B.; Curtiss, C. F.; Armstrong, R. C.; Hassager, O. *Dynamics of Polymeric Liquids. Kinetic Theory*, 2nd ed.; Wiley-Interscience: New York, 1987; Vol. 2.
(6) Buck, R. C. *Advanced Calculus*; McGraw-Hill: New York, 1978.
(7) des Cloizeaux, J.; Jannink, G. *Polymers in Solution: Their Modelling and Structure*; Oxford University Press: Oxford, 1990.
(8) Doi, M.; Edwards, S. F. *The Theory of Polymer Dynamics*; Oxford University Press: Oxford, 1986.
(9) Fixman, M. *J. Chem. Phys.* **1966**, *45*, 785, 793.
(10) Larson, R. G. *Constitutive Equations for Polymer Melts and Solutions*; Butterworth: Boston, 1988.
(11) Press, W. H.; Teukolsky, S. A.; Vetterling, W. T.; Flannery, B. P. *Numerical Recipes in FORTRAN*, 2nd ed.; Cambridge University Press: Cambridge, 1992.
(12) Öttinger, H. C. *J. Non-Newtonian Fluid Mech.* **1987**, *26*, 207.
(13) Öttinger, H. C.; Rabin, Y. *J. Non-Newtonian Fluid Mech.* **1989**, *33*, 53.
(14) Öttinger, H. C. *Phys. Rev.* **1989**, *A40*, 2664.
(15) Öttinger, H. C. *Stochastic Processes in Polymeric Fluids*; Springer: Berlin, 1996.
(16) Prakash, J. R. The Kinetic Theory of Dilute Solutions of Flexible Polymers: Hydrodynamic Interaction. In *Advances in the Flow and Rheology of Non-Newtonian Fluids*; Siginer, D. A., Kee, D. D., Chhabra, R. P., Eds.; Rheology Series; Elsevier Science: New York, in press.
(17) Schieber, J. D. *J. Rheol.* **1993**, *37*, 1003.
(18) Wagner, N. J.; Öttinger, H. C. *J. Rheol.* **1997**, *41*, 757.
(19) Wedgewood, L. E. *Rheol. Acta* **1993**, *32*, 405.
(20) Yamakawa, H. *Modern Theory of Polymer Solutions*; Harper and Row: New York, 1971.
(21) Zylka, W.; Öttinger, H. C. *J. Chem. Phys.* **1989**, *90*, 474.
(22) Zylka, W. *J. Chem. Phys.* **1991**, *94*, 4628.
(23) Zylka, W.; Öttinger, H. C. *Macromolecules* **1991**, *24*, 484.

MA981534B